Journal of the Korean Physical Society, Vol. 48, No. 4, April 2006, pp. 607∼613

Physical and Electrical Characteristics of Atomic-Layer-Deposited Hf-Silicate Thin Films Using $Hf[N(CH_3)(C_2H_5)]_4$ and $SiH[N(CH_3)_2]_3$ Precursors

K. B. Chung and C. N. Whang
Institute of Physics and Applied Physics, Yonsei University, Seoul 120-749

M.-H. Cho*
Nano Surface Group, Korea Research Institute of Standards and Science, Daejeon 305-600

C. J. Yim and D.-H. Ko
Department of Ceramics Engineering, Yonsei Universitiy, Seoul 120-749

Y.-S. Kim, M. J. Kim, J.-H. Lee and N. I. Lee
Advanced Process Development Team, System LSI Division, Samsung Electronics Co. Ltd., Yongin 449-711

(Received 24 January 2006)

Hf-silicate films were grown by using atomic layer deposition with $Hf[N(CH_3)(C_2H_5)]_4$ and $SiH[N(CH_3)_2]_3$ precursors. The composition of the Hf-silicate films was excellently well controlled by using the ratio of the deposition cycles of HfO_2 and SiO_2 (Hf/Si). The physical and the electrical characteristics of the Hf-silicate films were compared for Hf/Si = 3/1, Hf/Si = 1/1, and Hf/Si = 1/3. The relative Hf/(Hf+Si) compositions were 58 %, 41 %, and 25 % for Hf/Si = 3/1, Hf/Si = 1/1, and Hf/Si = 1/3, respectively. The binding characteristics of the Hf-silicate films were shifted in the direction of higher binding energy with increasing of SiO_2 portion, resulting in electric charging. The molecular structure of the Hf-silicate films was changed by the relative compositions of HfO_2 and SiO_2. In addition, the dielectric characteristics of the Hf-silicate films were directly proportional to the HfO_2 portion.

PACS numbers: 81.10.-h, 68.55.-a, 81.15.-z
Keywords: High-k dielectric, Hf-silicate, Atomic layer deposition

I. INTRODUCTION

As the sizes of silicon-based devices have been scaled down and lower power consumption has been required, the conventional SiO_2 gate dielectric thickness has been pushed below 15 Å for sub-micon complementary metal-oxide semiconductor (CMOS) transistors [1]. However, the shrinkage of gate dielectric thickness causes an increase in the leakage current through direct tunnelling across the gate dielectric [2]. For reducing the leakage current due to direct tunnelling, high dielectric constant (high-k) materials allow for an increase in the physical thickness while maintaining a low equivalent oxide thickness [3]. Various high-k materials, such as ZrO_2, HfO_2 and silicates of either Hf or Zr, have been considered as promising candidates to replace Si-based oxides [4–6]. Such materials should have high dielectric constants and satisfy thermal stability requirements, excluding interfacial reactions and structural changes after post-annealing treatment under the integration process. Unfortunately, most high dielectric oxide films do not have sufficient thermal stability because they easily undergo structural changes into poly-crystalline structures and can thermodynamically react with the Si substrate [7,8]. In order to enhance thermal stability, a number of studies have attempted to create silicate films or aluminate films by incorporating of SiO_2 and Al_2O_3 [5,9,10]. Among the many candidates, Hf-silicate films show superior interfacial stability in contact with Si and universal channel mobility [11]. Thus, the fabrication of compositionally controlled Hf-silicate films is very important to obtain optimized process conditions, which have the excellent characteristics in point of physical and electrical stability.

Atomic layer deposition (ALD) is a desirable technique for precise control of the composition, film thickness, conformality, and uniformity [12]. Hafnium tetrachloride ($HfCl_4$) was widely used as a Hf precursor for ALD Hf-based oxide film growth [13]. Recently, there

*E-mail: mhcho@kriss.re.kr

have been many reports using Hf-amide-type precursors such as $Hf[N(CH_3)(C_2H_5)]_4$ to solve the problem of particles or residual Cl obtained when using $HfCl_4$ [14]. Various Si precursors, such as $Si(OC_2H_5)_4$ and $NH_2(CH_2)_3Si(OC_2H_5)_3$, have been used to grow the Hf-silicate films [15, 16]. However, it is difficult to obtain SiO_2-rich Hf-silicate films because the deposition of SiO_2 is a very slow process. Furthermore, another additional process using $Al(CH_3)_3$ and H_2O prior to film deposition has been applied to accelerate SiO_2 deposition [16]. Therefore, the selection and combination of proper precursors are very important to deposit well-defined Hf-silicate films. Of many precursors, $Hf[N(CH_3)(C_2H_5)]_4$ is a good precursor because its melting point is very low (<–70 °C) and its vapor pressure is medium (0.5 Torr at 85 °C). Among the Si-amide-type precursors, $SiH[N(CH_3)_2]_3$ has very low melting point (<–90 °C), but a very high vapor pressure (25.4 Torr at 50 °C) [18]. Kim *et al.* reported electrical data for atomic-layer-deposited Hf silicate using $Hf[N(CH_3)(C_2H_5)]_4$ and new Si precursors for gate dielectric applications [17]. Kamiyama *et al.* fabricated Hf-silicate films using $Hf[N(CH_3)(C_2H_5)]_4$, $SiH[N(CH_3)_2]_3$ precursors and O_3 as the oxidant [18]. However, these reports focused on the fabrication of Hf-silicate films and a comparison of the dependences of the device characteristics on the Si precursors without a detailed study of the physical properties in relation to the composition of the Hf-silicate films.

In this study, we fabricated compositionally defined Hf-silicate films by controlling the number of alternate depositions in HfO_2 and SiO_2 with liquid precursors of $Hf[N(CH_3)(C_2H_5)]_4$ and $SiH[N(CH_3)_2]_3$. The physical and the electrical characteristics of the compositionally controlled Hf-silicate films were investigated by using several measurements. The properties of the Hf-silicate films were strongly affected by the compositions of HfO_2 and SiO_2 in the Hf-silicate films.

II. EXPERIMENT

Hf-silicate films were grown on (100)-orientated *p*-type Si wafers that had been cleaned chemically by using the standard Radio Corporation of America (RCA) method to remove organic and metallic residues [19]. After cleaning, the Si wafers were pre-processed to grow an interfacial layer of SiO_2 with a thickness of approximately 1.5 nm by using rapid thermal oxidation (RTO). The Hf-silicate films were deposited by means of an atomic layer deposition (ALD) system, which has a vertical warm-wall reactor with a shower head and a heated susceptor. The Hf-silicate films composed of HfO_2 and SiO_2 with 3 nm thicknesses were grown at a temperature of 280 °C by using Tetrakis(ethylmethylamino)Hf (TEMAHf: $Hf[N(CH_3)(C_2H_5)]_4$) and Tris(deimethylamino)silane (tDMAS: $SiH[N(CH_3)_2]_3$), as liquid precursors. Hf[N

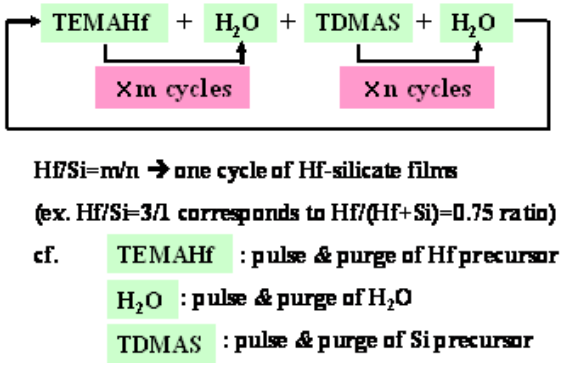

Fig. 1. A schematic diagram of ALD Hf-silicate deposition cycle. Hf/Si = m/n is one cycle of Hf-silicate films, composed m cycles of HfO_2 and n cycles of SiO_2.

$(CH_3)(C_2H_5)]_4$ and $SiH[N(CH_3)_2]_3$ were introduced to the ALD reactor using a liquid flow meter and liquid mass flow systems and were vaporized at 85 °C and 50 °C, respectively. Water vapor served as the oxygen agent, and nitrogen was supplied as the purge and carrier gas. In order to control the composition of the Hf-silicate films, we used a procedure in which one deposition cycle of Hf-silicate films (m+n) is composed of m cycles of HfO_2 and n cycles of SiO_2, as shown in the schematic diagram of Fig. 1. The growth rates of Hf-silicate films are 0.9 Å/cycle, 0.89 Å/cycle, and 2.52 Å/cycle for Hf/Si = 1/3, Hf/Si = 1/1, and Hf/Si = 3/1, respectively. A comparison of the physical and the electrical characteristics was performed with the Hf-silicate films whose relative ratios of deposition cycles, between HfO_2 and SiO_2, corresponded to Hf/Si = 3/1, Hf/Si = 1/1, and Hf/Si = 1/3, respectively.

The interfacial and the structural characteristics of compositionally controlled Hf-silicate films were investigated using medium energy ion scattering (MEIS). The kinematic scattering energy analysis gives elemental and quantified information in the depth direction. The MEIS analysis was accomplished with a 100-keV proton beam in the double-alignment condition, which reduced contributions from the crystalline Si substrates [20]. The electronic energy loss of 100-keV protons was precisely measured with an electrostatic energy analyzer. The incident ions were along the [111] direction, and the scattered ions were along the [001] direction, giving a scattering angle of 125°. Quantitative analysis of the different species was carried out with a depth resolution of 3 ∼ 5 Å in the near surface. During the MEIS experiments, the sample was exposed to a minimum H^+ beam dose in order to avoid damage caused by the beam.

In order to examine the dependence of the electronic structure of Hf-silicate films on the relative ratio of the deposition cycles between HfO_2 and SiO_2, we carried out the high-resolution X-ray photoelectron spectroscopy (HR-XPS) and near-edge X-ray absorption fine structure (NEXAFS) measurements at the Pohang accelerator lab-

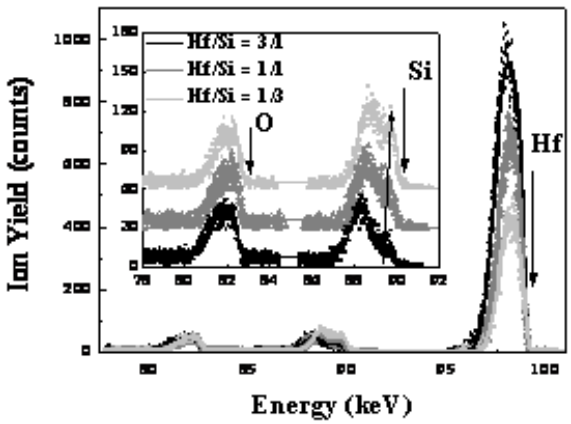

Fig. 2. MEIS energy spectra as a function of deposition cycle between HfO_2 and SiO_2 (Hf/Si). The solid dots are raw spectrum data and the solid lines are the fitted data. The inset shows the enlargement of the Si and O region. The arrow in the Si region indicates the increase of deposited Si in Hf silicate films.

oratory (PAL) on beamline 8A1, which is connected to an undulator and uses a third-generation synchrotron radiation source. Photoelectrons were detected with a pass energy of 15 eV (energy resolution less than 0.15 eV). The binding energy was calibrated with reference to the position of bulk Si $2p_{3/2}$ levels at $E_b = 99.2$ eV for the energy of each photon. The energy of the incident photons was fixed at 650 eV, thus providing a high photoionization cross-section of Hf $4f$, Si $2p$, and O $1s$. Gaussian-Lorentzian line shapes were used for deconvolution after standard Shirley background subtraction. The dielectric characteristics related to the compositional variations were measured by using metal-oxide-semiconductor (MOS) capacitors with Pt electrodes produced by using a sputtering method with a shadow mask. The average size of the Pt electrodes was $\sim 3.5 \times 10^{-4}$ cm^2, as shown by microscope measurements. Capacitance-voltage (C-V) measurements were performed using the HP4284A instrument at high frequency (1 MHz).

III. RESULTS AND DISCUSSION

Fig. 2 shows the backscattering energy spectra of Hf-silicate films, measured by using MEIS, as a function of the deposition cycles between HfO_2 and SiO_2 (Hf/Si). As the portion of HfO_2 deposition cycles of the Hf-silicate films increases, the intensity and the area of the Hf peak (∼99 keV), which indicate the quantity of deposited Hf, increases linearly. The quantity of deposited Si near ∼90 keV similarly increases as the portion of SiO_2 deposition cycles of the Hf-silicate films increases, as shown in the inset of Fig. 2. On the other hand, the O peaks have the same shapes and widths, regardless of the ratio of deposition cycles between HfO_2 and SiO_2, resulting in the same total thickness. The thickness of the Hf-silicate films for all combinations of the deposition cycles between HfO_2 and SiO_2 is approximately ∼4.5 nm, which was calculated from the energy deviation of the O peak. Thus, these tendencies of the MEIS spectra show that the composition of Hf-silicate films is excellently controlled by using the ratio of alternate depositions of HfO_2 and SiO_2.

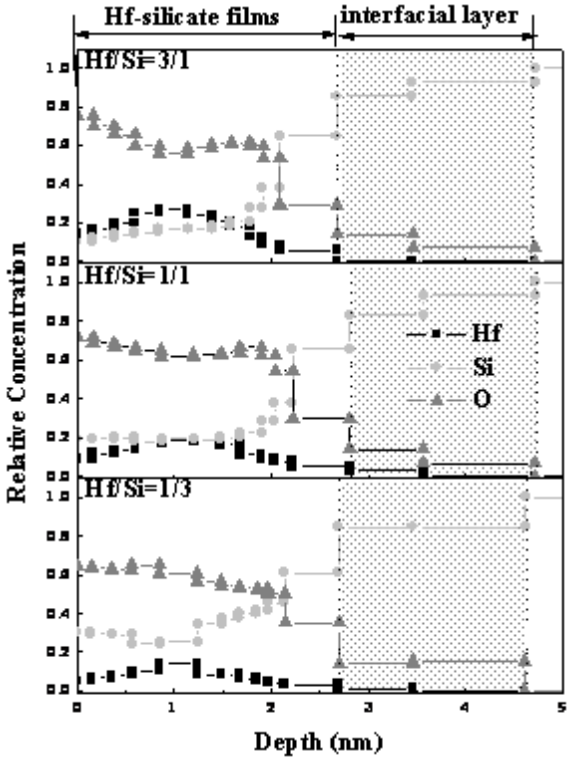

Fig. 3. Compositional depth profiles as a function of deposition cycle between HfO_2 and SiO_2 (Hf/Si).

For further information on the relative concentrations in the depth direction, MEIS spectra were simulated using the Kido program [21]. Fig. 3 shows the compositional depth profile as a function of deposition cycles between HfO_2 and SiO_2 (Hf/Si). The total thickness of Hf-silicate films, including an ∼1.7 nm thick interfacial layer, is 4.6 nm ∼ 4.7 nm for all samples, which coincided with the calculated value (∼4.5 nm) from the MEIS energy spectra shown in Fig. 2. Fig. 4 shows the changes of Hf coverage and Si coverage on the Hf/(Hf+Si) ratio. The coverages of Hf, which indicates the amounts of Hf in the Hf-silicate films, linearly increased: 1.4×10^{15}, 2.4×10^{15}, and 3.3×10^{15} Hf atom/cm^2 for Hf/Si = 1/3, Hf/Si = 1/1, and Hf/Si = 3/1, respectively. With the amount of Si in the Hf-silicate films, except the Si of the interfacial layer (∼1.7 nm) on the Si substrate, the Hf coverages linearly decreased: 4.3×10^{15}, 3.4×10^{15}, and 2.4×10^{15} Si atom/cm^2 for Hf/Si = 1/3, Hf/Si = 1/1, and Hf/Si = 3/1, respectively. Fig. 5 shows the

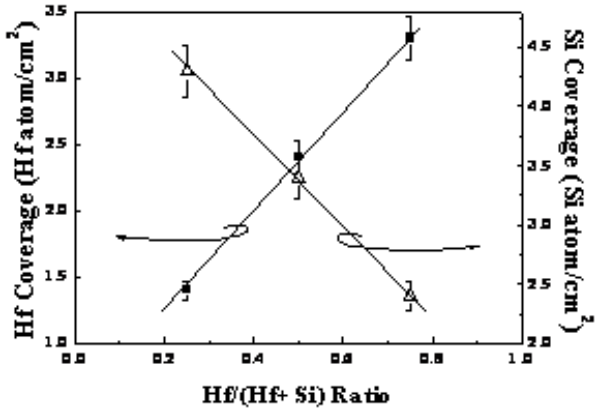

Fig. 4. The changes of Hf coverage and Si coverage in ALD Hf-silicate films on the number of Hf/(Hf+Si) ratios.

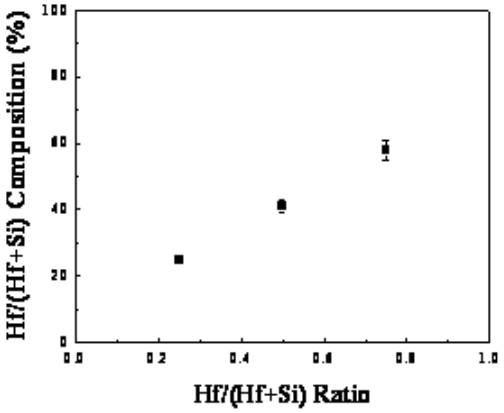

Fig. 5. The Hf/(Hf+Si) compositions in ALD Hf-silicate films on the number of Hf/(Hf+Si) ratio.

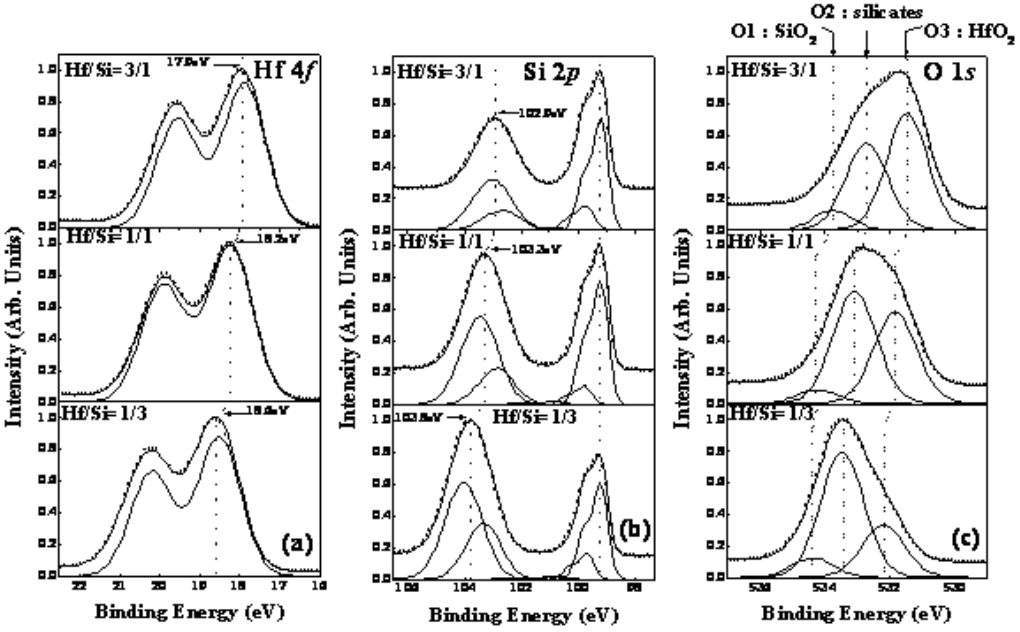

Fig. 6. XPS spectra of (a) Hf $4f$, (b) Si $2p$, and (c) O $1s$ as a function of deposition cycle between HfO_2 and SiO_2 (Hf/Si). O_1, O_2, and O_3 in (c) indicate SiO_2, silicates, and HfO_2, respectively.

dependence of the Hf/(Hf+Si) compositions of the Hf-silicate films on the number of Hf/(Hf+Si) ratio. The relative Hf/(Hf+Si) compositions for the Hf-silicate films are 58 %, 41 %, and 25 % for Hf/Si = 3/1, Hf/Si = 1/1, and Hf/Si = 1/3, respectively. This suggests that the Hf/(Hf+Si) composition can be easily controlled by using the Hf/Si deposition-cycle ratio.

Fig. 6 shows Hf $4f$, Si $2p$, and O $1s$ core level spectra of 2-nm-thick Hf-silicate films as a function of the deposition cycles between HfO_2 and SiO_2 (Hf/Si). In the Hf spectra in Fig. 6 (a), although the binding-energy shifts are different to some degree, the binding energies for all Hf-silicate films are shifted to higher energy compared to the binding energy in pure HfO_2 ($\sim$17 eV). As the portion of SiO_2 deposition cycles increases, the intensity of the Si peak related to SiO_2 and silicates increases in comparison with the intensity of the main peak of the bulk, Si $2p_{3/2}$, as shown in Fig. 6 (b). The spectra of O have a similar tendency to the spectra of Si. The O_1, $_2$, and O_3 peaks indexed in Fig. 6 (c) could be carefully assigned to SiO_2, silicates, and HfO_2 by deconvoluting the O peak, excluding the higher binding shift of the O peak with the portion of SiO_2 deposition cycles [22]. The intensity of the O_3 peak indicates HfO_2 increases with the portion of HfO_2 deposition cycles. On the other hand, the intensity of the O_2 peak indicates silicates increase with the portion of SiO_2 deposition cycles. The compositional characteristics of Hf-silicate films as a function of ratio of deposition cycles between HfO_2 and SiO_2 was also confirmed through the XPS spectra of various elements. Another important finding is that the core-level spectra of all elements are shifted to higher binding en-

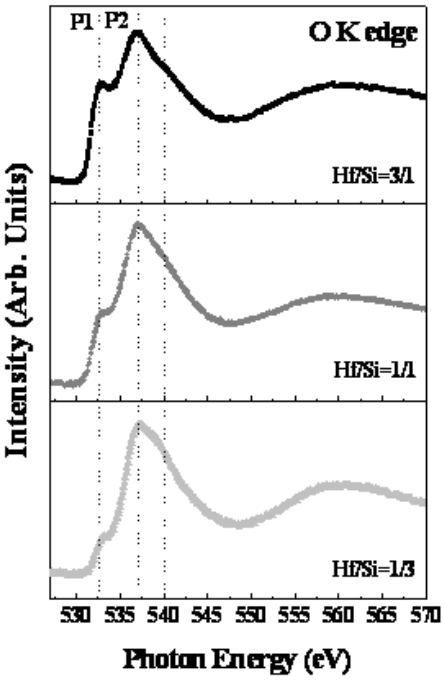

Fig. 7. NEXAFS spectra of the O K edge as a function of deposition cycle between HfO_2 and SiO_2 (Hf/Si). Dotted lines indicate P1: e_g (Hf 5d + O 2pσ) and P2: t_{2g} (Hf 5d + O 2pπ), respectively.

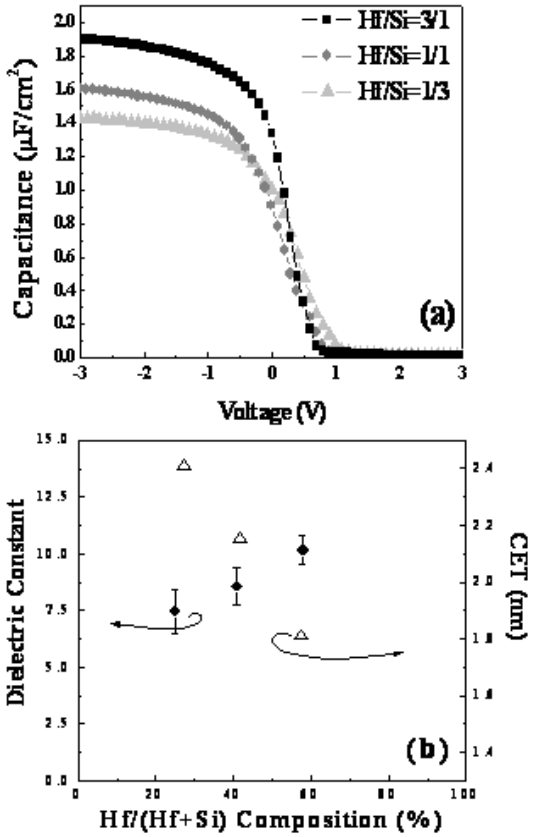

Fig. 8. (a) C-V curves as as a function of deposition cycle between HfO_2 and SiO_2 (Hf/Si). (b) Dielectric constant and capacitance equivalent oxide thickness (CET) depending on the relative Hf/(Hf+Si) composition.

ergy with increasing portion of SiO_2 deposition cycles. Previous research has been reported that the formation of a Hf-silicate layer at the interfacial region causes a higher binding-energy shift in the Hf peak and a lower binding-energy shift in the Si peak. The reason for the peak shift in the Hf-silicate layer is thought to be due to the contributions of charge transfer and electrostatic effects; *i.e.*, considering the mixing of HfO_2 and SiO_2 to form a complex mixed oxides such as Hf-silicate films, more ionic HfO_2 would be expected to become even more ionic after the formation of the complex oxides whereas, neglecting Madelung and relaxation effects, the Si of the more covalent oxide should experience a corresponding covalence [23,24]. Thus, from the charge transfer model, the Hf peak is shifted to higher binding energy while the Si peak is shifted in the opposite direction. However, no difference in shift direction between Hf and Si is observed from our results as a function of the portion of deposition cycles between HfO_2 and SiO_2. All elemental peaks shift in the direction of higher binding energy as the portion of SiO_2 deposition cycles increases. The consistent shift to higher binding energy with increasing portion of SiO_2 deposition cycles is very similar to the energy shift in the case of the SiO_2 films depending on the SiO_2 film thickness [25]. A considerable chemical shift can be produced by electric charging due to X-ray irradiation, contributing to the dependence on the portion of SiO_2, as in our previous report [26]. In addition, the insulating properties depend on the portion of SiO_2 because the band gap for SiO_2 (∼8.9 eV) is much larger than that for HfO_2 (∼5.6 eV). Therefore, the difference in insulating properties with the ratio of deposition cycles between HfO_2 and SiO_2 affects electric charging, resulting in a peak shift.

NEXAFS analysis is a sensitive method to detect changes in molecular structure with relation to the compositions of HfO_2 and SiO_2 in Hf-silicate films. The O K-edge of Hf-silicate films can be represented as a superposition of both features due to a complex mixing of HfO_2 and SiO_2 [27, 28]. Fig. 7 presents the O K-edge spectra as a function of the portion of deposition cycles between HfO_2 and SiO_2 (Hf/Si). The distinct finding that depends on the ratio of HfO_2 and SiO_2 deposition cycles is the changes in representative peaks, such as P1 and P2, indexed in Fig. 7. As the portion of HfO_2 deposition cycles increases, the intensity of the P1 peak increases whereas that of the P2 peak relatively decreases. On the contrary, as the portion of SiO_2 deposition cycles increases, the intensity of the P1 peak decreases and that of P2 peak increases. These tendencies have the following explanations. The O K-edge of HfO_2 is related to the oxygen p-projected density of states, which consists of four representative unoccupied hybridized states

under an assumption of octahedral symmetry: P1: e_g (Hf 5d + O 2pσ), P2: t_{2g} (Hf 5d + O 2pπ), and (a_{1g} + t_{1u})(Hf 6sp + O 2p) [27, 29]. The incorporation of SiO_2 in the unoccupied hybridized orbitals of HfO_2 may be caused by a modification of the O K-edge spectrum for HfO_2 due to the overlap of the O K-edge spectrum for SiO_2 with a double band caused by O p-states hybridized with Si 3sp states, which is coincident with the energy position of the P2 peak.[27] Therefore, the molecular structures of Hf-silicate films are also modified by the compositions of HfO_2 and SiO_2.

Finally, the electrical characteristics of Hf-silicate films as a function of the portion of the deposition cycles between HfO_2 and SiO_2 (Hf/Si) were measured in a MOS cap with a Pt electrode, as shown in Fig. 8 (a). As the portion of HfO_2 deposition cycles increases, the accumulation capacitance increases. This is caused by the difference in dielectric constants between HfO_2 (∼20) and SiO_2 (∼3.9). Fig. 8 (b) shows the changes in dielectric constant and capacitance equivalent oxide thickness (CET) with the relative Hf/(Hf+Si) composition. The dielectric constant was calculated from the total accumulation capacitance by assuming that the only dielectric layer included Hf-silicate films and an interfacial layer. The thickness of the Hf-silicate films is based on the MEIS depth profile data, as shown in Fig. 3. The dielectric constant of Hf-silicate films is directly proportional to the portion of HfO_2 in Hf-silicate films. The CET is the thickness of a SiO_2 layer that would give the same capacitance density as that provided by a given dielectric layer or a stack of dielectric layers without quantum corrections. The CET can be obtained by solving for CET $= \varepsilon_0 \times A \times 3.9/C_{acc}$, where C_{acc} is the accumulation capacitance, ε_0 is the permittivity of vacuum, and A is the area of the electrode. The CET values are 1.81, 2.15, and 2.41 nm for Hf/Si = 3/1, Hf/Si = 1/1, and Hf/Si = 1/3, respectively. The CET linearly decreases with increasing Hf/(Hf+Si) composition, as shown in Fig. 8 (b). This means that a thinner equivalent oxide thickness can be obtained by increasing the HfO_2 portion in Hf-silicate films and that the compositions of HfO_2 and SiO_2 are strongly related to the dielectric properties of Hf-silicate films.

IV. CONCLUSIONS

We studied Hf-silicate films grown by using ALD with $Hf[N(CH_3)(C_2H_5)]_4$ and $SiH[N(CH_3)_2]_3$ precursors. The ratio of alternate deposition cycles between HfO_2 and SiO_2 could be used to control the composition of the Hf-silicate films. The binding characteristics of the Hf-silicate films shifted in the direction of higher binding energy with increasing of SiO_2 portion, resulting in electric charging. The characteristics of the molecular structure for Hf-silicate films changed with the relative compositions of HfO_2 and SiO_2. In addition, the electrical characteristics, such as the accumulated capacitance and the dielectric constant, are directly proportional to the portion of HfO_2 in the Hf-silicate films.

ACKNOWLEDGMENTS

This work was partially supported by the National Program for Tera-level Nanodevices and System IC 2010. We gratefully acknowledge the technical advice of H. J. Shin and M.-C. Jung in Pohang Accelerator Laboratory (PAL) on beamline 8A1.

REFERENCES

[1] Angus I. Kingon, Jon-Paul Maria and S. K. Streiffer, Nature **406**, 1032 (2000).
[2] G. D. Wilk and R. W. Wallace, Appl. Phys. Lett. **76**, 112 (2000).
[3] R. M. Wallace and G. D. Wilk, Crit. Rev. Solid. State. **28**, 231 (2003).
[4] M. -H. Cho, Y. S. Roh, C. N. Whang, K. Jeong, H. J. Choi, S. W. Nam, D. -H. Ko, J. H. Lee, N. I. Lee and K. Fujihara, Appl. Phys. Lett. **81**, 1071 (2002).
[5] G. D. Wilk, R. M. Wallace and J. M. Anthony, J. Appl. Phys. **87**, 484 (2000).
[6] Hyoungsub Kim and Paul C. McIntyre, J. Korean Phys. Soc. **48**, 5 (2006).
[7] M. Copel, M. Gribelyuk and E. Gusev, Appl. Phys. Lett. **76**, 436 (2000).
[8] H. Kim, P. C. McIntyre and K. C. Saraswat, Appl. Phys. Lett. **82**, 106 (2003).
[9] M.-Y. Ho, H. Gong, G. D. Wilk, B. W. Busch, M. L. Green, W. H. Lin, A. See, S. K. Lahiri, M. E. Loomans, Petri I. Raisanen and T. Gustafsson, Appl. Phys. Lett. **81**, 4218 (2002).
[10] H. Takeuchi and T.-J. King, Appl. Phys. Lett. **83**, 788 (2003).
[11] H. Watanabe, M. Saitoh, N. Ikarashi and T. Tatsumi, Appl. Phys. Lett. **85**, 449 (2004).
[12] T. Suntola, Thin Solid Films **216**, 84 (1992).
[13] H. S. Chang, H. Hwang, M.-H. Cho and D. W. Moon, Appl. Phys. Lett. **86**, 031906 (2005).
[14] X. Liu, S. Ramanthan, A. Longdergan, A. Srivastava, E. Lee, T. E. Seidel, J. T. Barton, D. Pang and R. G. Gordon, J. Electrochem. Soc. **152**, G213 (2005).
[15] K. Kukli, Mikko Ritala, Markku Leskela, Timo Sajavaara, Juhani Keinonen, Rama I. Hegde, David C. Gilmer and Philip J. Tobin, J. Electrochem. Soc. **151**, F98 (2004).
[16] Z. M. Rittersma, F. Roozeboom, M. A. Verheijen, J. G. M. van Berkum, T. Dao, J. H. M. Snijders, E. Vainonen-Ahlgren, E. Tois, M. Tuominen and S. Haukka, J. Electrochem. Soc. **151**, C716 (2004).
[17] Yun-Seok Kim, *et al.*, Tech. Dig. -Int. Electron Device Meet. 511 (2004).
[18] S. Kamiyama, T. Miura, Y. Nara and T. Arikado, Electrochem. Solid-State Lett. **8**, G215 (2005).
[19] W. Keren, RCA Rev. **31**, 207 (1970).

[20] J. F. van der Veen, Sur. Sci. Rep. **5**, 199 (1985).
[21] Y. Kido and T. Koshikwa, J. Appl. Phys. **67**, 187 (1990).
[22] Y. Q. Wang, J. H. Chen, W. J. Woo, Y.-C. Yeo, A. Chin and A. Y. Du, J. Appl. Phys. **98**, 013536 (2005).
[23] M. J. Guittet, J. P. Crocombette and M. Gautier-Soyer, Phys. Rev. B **63**, 125117 (2001).
[24] O. Renault, D. Samour, J.-F. Damlencourt, D. Blin, F. Martin, S. Marthon, N. T. Barrett and P. Besson, Appl. Phys. Lett. **81**, 3627 (2002).
[25] S. Iwata and A. Ishizaka, J. Appl. Phys. **79**, 6653 (1996).
[26] M.-H. Cho, K. B. Chung, C. N. Whang, D. W. Lee and D.-H. Ko, Appl. Phys. Lett. **87**, 242906 (2005).
[27] S. Ramanathan, P. C. McIntyre, J. Luning, P. S. Lysaght, Y. Yang, Z. Chen and S. Stemmer, J. Electrochem. Soc. **150**, F173 (2003).
[28] N. Ikarashi and K. Manabe, J. Appl. Phys. **94**, 480 (2003).
[29] L. Soriano, M. Abbate, J. C. Fuggle, M. A. Jimenez, J. M. Sanz, C. Mythen and H. A. Padmore, Solid State Commun. **87**, 699 (1993).